

Somersault by Stokes

Yongheng Zhang

6.14.2024

Although the various theorems under the general title of Stokes were motivated by classical theories in physics [3], once formulated and proved, they took on independent mathematical meanings, and thus could be applied in new contexts. This note discusses one such application in the kinematics of human motion in free fall and during space walk [2][1]. In particular, under the assumption of zero-sum angular momentum, Stokes' Theorems can help us design choreographic sequences for 2D stick figures to perform somersaults.

Classical Stokes' Theorem

We first consider the classical 3D Stokes' Theorem, in the format commonly found in calculus textbooks:

$$\int_{\partial S} \mathbf{F} \cdot d\mathbf{r} = \iint_S \nabla \times \mathbf{F} \cdot d\mathbf{S}. \quad (1)$$

In our application, the differential form $\mathbf{F} \cdot d\mathbf{r}$ models the infinitesimal change of the orientation angle θ , which will be proved in Theorem 2 to depend only on the three local angles α_1, α_2 , and α_3 , at the shoulder, hip, and knee of the stick figure in Figure 1, whose left and right limbs move synchronously. The stick figure is modeled as a linkage consisting of four uniform bars, corresponding to the arm, torso, thigh, and lower leg, with length l_i , mass m_i , counterclockwise oriented global angle θ_i , and moment of inertia $I_i = \frac{1}{12}m_i l_i^2$ about individual center of mass, labeled by $i = 1, 0, 2$, and 3, respectively. The head, neck, hand, and foot were also drawn in Figure 1 for better graphical representation.

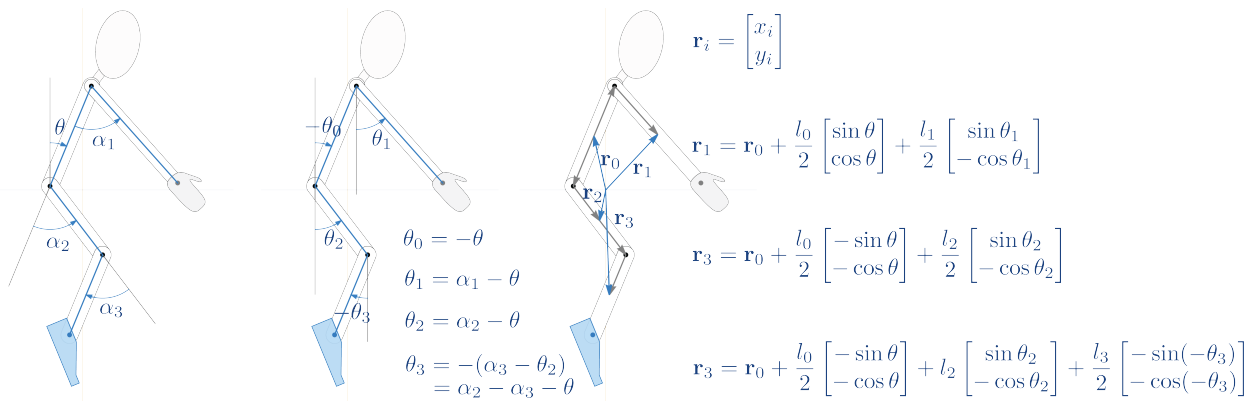


Figure 1: Definition of θ , α_i , $i = 1, 2, 3$, and θ_i , \mathbf{r}_i , $i = 0, 1, 2, 3$.

The origin of the planar coordinate system is at the total center of mass of the stick figure. Each position vector \mathbf{r}_i points from the origin to the center of mass (midpoint) of each bar. Thus, $\sum_{i=0}^3 m_i \mathbf{r}_i = \mathbf{0}$, from which we can solve for \mathbf{r}_0 . After substituting this \mathbf{r}_0 back into \mathbf{r}_i , we see that each \mathbf{r}_i is a linear combination of the four vectors

$$\begin{bmatrix} \sin \theta \\ \cos \theta \end{bmatrix}, \begin{bmatrix} \sin(\alpha_1 - \theta) \\ -\cos(\alpha_1 - \theta) \end{bmatrix}, \begin{bmatrix} \sin(\alpha_2 - \theta) \\ -\cos(\alpha_2 - \theta) \end{bmatrix}, \text{ and } \begin{bmatrix} \sin(\alpha_2 - \alpha_3 - \theta) \\ -\cos(\alpha_2 - \alpha_3 - \theta) \end{bmatrix}. \quad (2)$$

Lemma 1. For each $i = 0, 1, 2, 3$, $\frac{\partial x_i}{\partial \theta} = y_i$, and $\frac{\partial y_i}{\partial \theta} = -x_i$.

Proof. The above two equalities hold for the x and y components in the four vectors of (2). Thus, they also hold for x_i and y_i in \mathbf{r}_i , a linear combination of the vectors in (2). \square

The total angular momentum \mathbf{L} of the stick figure about its center of mass during free fall and space walk (no external force except gravity) is defined as $\sum_{i=0}^3 (\mathbf{r}_i \times m_i \dot{\mathbf{r}}_i + I_i \dot{\theta} \mathbf{k})$, where \mathbf{r}_i are considered vectors in \mathbb{R}^3 with the third component 0 and \mathbf{k} points out of the page. It can be shown by integrating equalities obtained from Newton's second and third laws that $\dot{\mathbf{L}} = \mathbf{0}$. Thus, \mathbf{L} is a constant, and we require it to be zero, which is summarized as

$$\sum_{i=0}^3 (m_i (x_i \dot{y}_i - y_i \dot{x}_i) + I_i \dot{\theta}_i) = 0. \quad (3)$$

Assuming that θ and α_i , $i = 1, 2, 3$ change with respect to t smoothly, then the following holds.

Theorem 2. There are functions $P(\alpha_1, \alpha_2, \alpha_3)$, $Q(\alpha_1, \alpha_2, \alpha_3)$, and $R(\alpha_1, \alpha_2, \alpha_3)$ continuously differentiable on the entire \mathbb{R}^3 such that

$$\dot{\theta} = P(\alpha_1, \alpha_2, \alpha_3) \dot{\alpha}_1 + Q(\alpha_1, \alpha_2, \alpha_3) \dot{\alpha}_2 + R(\alpha_1, \alpha_2, \alpha_3) \dot{\alpha}_3. \quad (4)$$

Proof. By the chain rule, $\dot{x}_i = \frac{\partial x_i}{\partial \theta} \dot{\theta} + \sum_{i=1}^3 \frac{\partial x_i}{\partial \alpha_i} \dot{\alpha}_i$ and $\dot{y}_i = \frac{\partial y_i}{\partial \theta} \dot{\theta} + \sum_{i=1}^3 \frac{\partial y_i}{\partial \alpha_i} \dot{\alpha}_i$. Then (3) becomes

$$T(\theta, \alpha_1, \alpha_2, \alpha_3) \dot{\theta} + A(\theta, \alpha_1, \alpha_2, \alpha_3) \dot{\alpha}_1 + B(\theta, \alpha_1, \alpha_2, \alpha_3) \dot{\alpha}_2 + C(\theta, \alpha_1, \alpha_2, \alpha_3) \dot{\alpha}_3 = 0,$$

where

$$\begin{aligned} T(\theta, \alpha_1, \alpha_2, \alpha_3) &= \sum_{i=0}^3 m_i (x_i \frac{\partial y_i}{\partial \theta} - y_i \frac{\partial x_i}{\partial \theta}) - I_0 - I_1 - I_2 - I_3, \\ A(\theta, \alpha_1, \alpha_2, \alpha_3) &= \sum_{i=0}^3 m_i (x_i \frac{\partial y_i}{\partial \alpha_1} - y_i \frac{\partial x_i}{\partial \alpha_1}) + I_1, \\ B(\theta, \alpha_1, \alpha_2, \alpha_3) &= \sum_{i=0}^3 m_i (x_i \frac{\partial y_i}{\partial \alpha_2} - y_i \frac{\partial x_i}{\partial \alpha_2}) + I_2 + I_3, \\ C(\theta, \alpha_1, \alpha_2, \alpha_3) &= \sum_{i=0}^3 m_i (x_i \frac{\partial y_i}{\partial \alpha_3} - y_i \frac{\partial x_i}{\partial \alpha_3}) - I_3. \end{aligned}$$

By Lemma 1, $T < 0$ on \mathbb{R}^3 . Using Lemma 1 again and Clairaut's Theorem on the equality of mixed second order partial derivatives, we also see that $\frac{\partial T}{\partial \theta} = \frac{\partial A}{\partial \theta} = \frac{\partial B}{\partial \theta} = \frac{\partial C}{\partial \theta} = 0$. Thus, all four functions T , A , B , and C depend on α_i , $i = 1, 2, 3$ only. Then, setting $P = -A/T$, $Q = -B/T$ and $R = -C/T$ concludes the proof. \square

Letting $\langle \alpha_1(t), \alpha_2(t), \alpha_3(t) \rangle$ parametrize a curve C in \mathbb{R}^3 , and integrating (4) with respect to t , we see that the total angle change $\Delta\theta = \int_C P d\alpha_1 + Q d\alpha_2 + R d\alpha_3$, which depends on C but is independent of t . When C is closed, an orientable surface $S = \bigcup_{k=1}^N S_k$ can be found (even if C is knotted [6]) such that $C = \partial S$, and by (1) this line integral can be written as the following double integral, where each surface S_k is parametrized by $(u, v) \in D_k$, and $U = \frac{\partial R}{\partial \alpha_2} - \frac{\partial Q}{\partial \alpha_3}$, $V = \frac{\partial P}{\partial \alpha_3} - \frac{\partial R}{\partial \alpha_1}$, $W = \frac{\partial Q}{\partial \alpha_1} - \frac{\partial P}{\partial \alpha_2} \cdot \frac{\partial(\alpha_i, \alpha_j)}{\partial(u, v)}$ are Jacobian determinants.

$$\pm \sum_{k=1}^N \iint_{D_k} U \frac{\partial(\alpha_2, \alpha_3)}{\partial(u, v)} + V \frac{\partial(\alpha_3, \alpha_1)}{\partial(u, v)} + W \frac{\partial(\alpha_1, \alpha_2)}{\partial(u, v)} dA \quad (5)$$

We would like to find a suitable C achieving a relatively large $\Delta\theta$ by analyzing this double integral. For concreteness, we have chosen $l_0 = 2.5$, $l_1 = 3$, $l_2 = l_3 = 2$, $m_0 = 1$, $m_1 = 1/4$, $m_2 = m_3 = 1/2$, and the 3D cube domain $(\alpha_1, \alpha_2, \alpha_3) \in [0, \pi] \times [0, \frac{5}{6}\pi] \times [0, \frac{5}{6}\pi]$. For each value of $\alpha_1 \in [0, \pi]$ considered as the parameter, the graph of $U(\alpha_1, \alpha_2, \alpha_3)$ versus (α_2, α_3) was plotted. The overlaid graphs were shown in Figure 2(a), where the "sea level" reference plane was also shown. The overlaid graphs for $V(\alpha_1, \alpha_2, \alpha_3)$ and $W(\alpha_1, \alpha_2, \alpha_3)$ with parameters α_2 and α_3 , respectively, were shown in Figure 2(b) and 2(c).

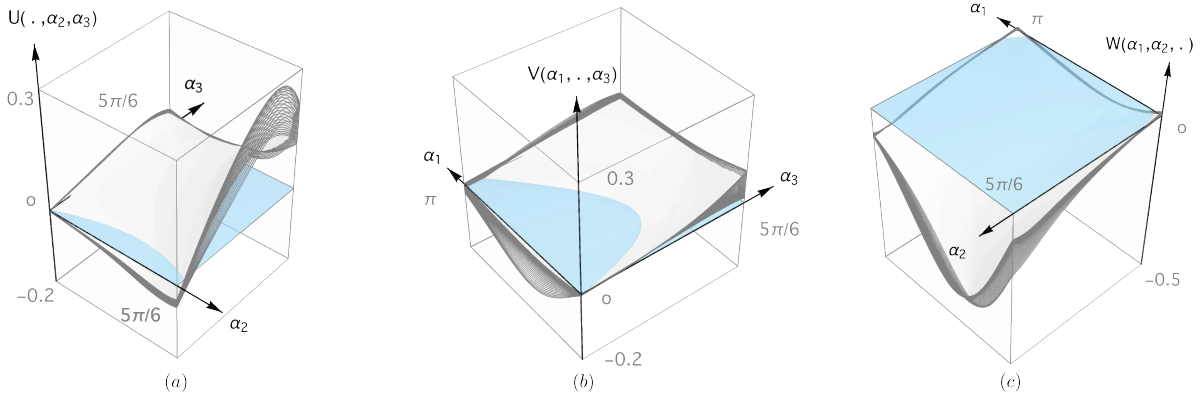


Figure 2: Overlaid graphs for each of $U(\cdot, \alpha_2, \alpha_3)$, $V(\alpha_1, \cdot, \alpha_3)$, and $U(\alpha_1, \alpha_2, \cdot)$.

For each of U , V , and W , its graph as the parameter changes more or less maintains the same shape, and W bounds the largest volume, followed by U , while V would have the least influence on (5). Thus, we could choose C such that it projects to a large clockwise loop on the (α_1, α_2) plane, and a large counterclockwise loop avoiding the blue strip along the α_2 axis on the (α_2, α_3) plane. Furthermore, recall that α_2 and α_3 are the angles at the hip and the knee (See Figure 1). Thus, once α_2 increases past $\frac{1}{2}\pi$ to its maximal value $\frac{5}{6}\pi$, it would be natural for α_3 to increase in parallel. Thus, with simplicity also in mind, a four-segment C was chosen in Figure 3(a), which bounds two surfaces S_1 and S_2 , parametrized by $(\alpha_1, \alpha_2, \alpha_3) = (\alpha_1, \alpha_2, \frac{5}{6}\alpha_1)$ with $D_1 : 0 \leq \alpha_1 \leq \pi, 0 \leq \alpha_2 \leq \frac{5}{6}\alpha_1$, and $(\alpha_1, \alpha_2, \alpha_3) = (\alpha_1, \alpha_2, \alpha_2)$ with $D_2 : 0 \leq \alpha_2 \leq \frac{5}{6}\pi, 0 \leq \alpha_1 \leq \frac{6}{5}\alpha_2$, respectively.

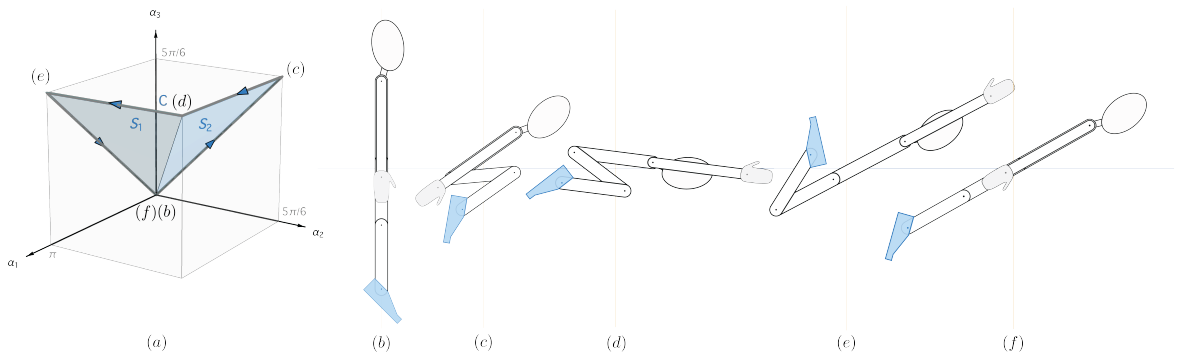


Figure 3: Path C , surfaces S_1 and S_2 , and five configurations of the stick figure during one cycle.

Thus, (5) becomes

$$\int_0^\pi \int_0^{\frac{5}{6}\alpha_1} \frac{5}{6}U(\alpha_1, \alpha_2, \frac{5}{6}\alpha_1) - W(\alpha_1, \alpha_2, \frac{5}{6}\alpha_1) d\alpha_2 d\alpha_1 + \int_0^{\frac{5}{6}\pi} \int_0^{\frac{6}{5}\alpha_2} V(\alpha_1, \alpha_2, \alpha_2) - W(\alpha_1, \alpha_2, \alpha_2) d\alpha_1 d\alpha_2, \quad (6)$$

whose numerical value is $1.05904\dots \text{ rad} \approx 60.68^\circ$, with contributions of 14.57%, 7.54%, and 77.89% from U , V , and W , respectively. Thus, if C is traversed 6 times before a small adjust, then the stick figure will turn 360° , thereby completing a somersault. See <https://youtu.be/NLIOnEloKuQ> for an animation.

Generalized Stokes' Theorem

In general, if the stick figure consists of $n + 1$ rods with $n \geq 2$ internal angles $\alpha_1, \dots, \alpha_n$, then we also have

$$\dot{\theta} = \sum_{j=1}^n P_j(\alpha_1, \dots, \alpha_n) \dot{\alpha}_j, \quad (7)$$

for functions P_j continuously differentiable on \mathbb{R}^n . Then by the generalized Stokes' Theorem [5], for closed curve C which bounds an oriented surface $S = \bigcup_{k=1}^N S_k$ in \mathbb{R}^n , we have

$$\int_C \sum_{j=1}^n P_j d\alpha_j = \pm \sum_{k=1}^N \iint_{S_k} \sum_{j=1}^n \sum_{i=1}^n \frac{\partial P_j}{\partial \alpha_i} d\alpha_i \wedge d\alpha_j = \pm \sum_{k=1}^N \iint_{D_k} \sum_{1 \leq i < j \leq n} U_{ij} \frac{\partial(\alpha_i, \alpha_j)}{\partial(u, v)} dA, \quad (8)$$

where S_k is parametrized by $(u, v) \in D_k$ and $U_{ij} = \frac{\partial P_j}{\partial \alpha_i} - \frac{\partial P_i}{\partial \alpha_j}$.

As an example, we start from the stick figure in the previous section, and then decompose the torso with length 2.5 and mass 1 into a thorax with length 1.5 and mass 0.6 and an abdomen with length 1 and mass 0.4. The global angle θ still goes from the upward pointing vertical direction to the thorax, and the extra variable α_4 describes the local angle at the waist, with value 0 for straightened torso. We set the domain be a 4D cube $(\alpha_1, \alpha_2, \alpha_3, \alpha_4) \in [0, \pi] \times [0, \frac{1}{2}\pi] \times [0, \frac{5}{6}\pi] \times [0, \frac{1}{2}\pi]$. Due to the flexibility at the waist, the configuration $\alpha_2 = \alpha_4 = \frac{1}{2}\pi$, $\alpha_3 = \frac{5}{6}\pi$ is attainable. Overlaid colorful graphs for the six functions U_{ij} versus (α_i, α_j) are shown in Figure 4, in which each parameter pair $(\alpha_{k_1}, \alpha_{k_2})$ where $k_1, k_2 \neq i, j$ corresponds to a color, which in turn labels a graph. We use a 2D subspace of the RGB color space where blue level is full while the first and second parameters α_{k_1} and α_{k_2} are aligned with red and green, respectively.

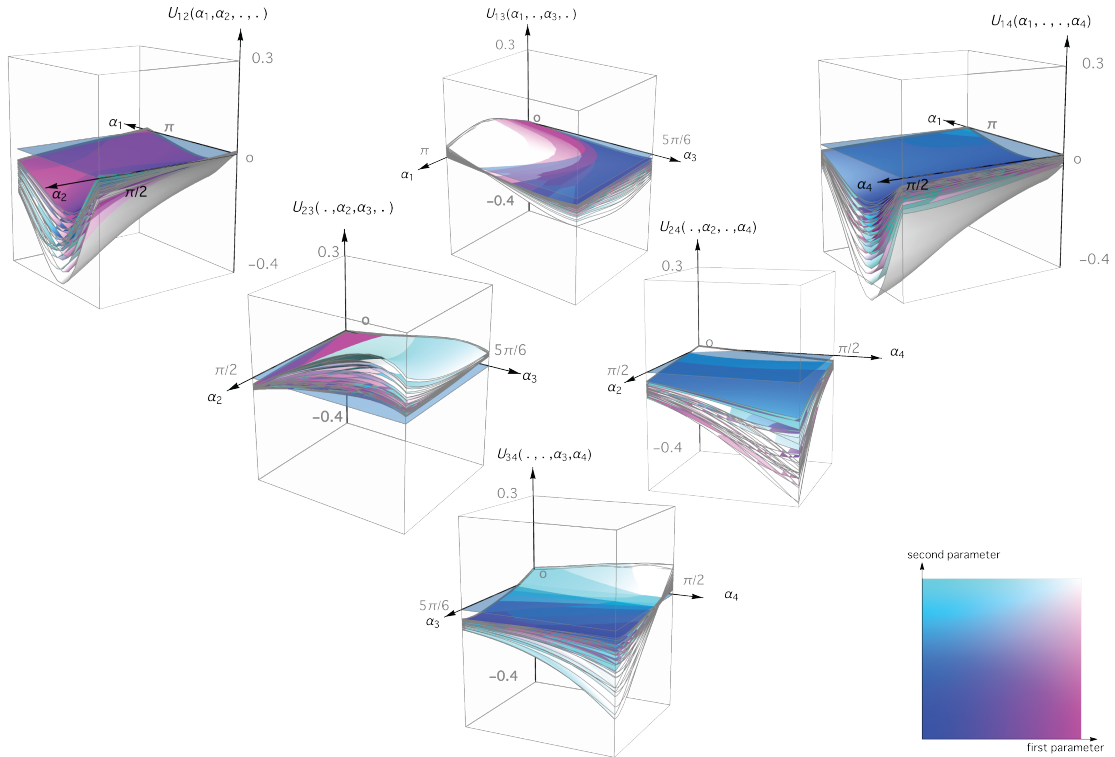


Figure 4: Overlaid graphs for each U_{ij} versus (α_i, α_j) while the other two variables are color parameters.

We observe that $U_{12}(\alpha_1, \alpha_2, \frac{5}{6}\pi, \frac{1}{2}\pi)$ and $U_{14}(\alpha_1, \frac{1}{2}\pi, \frac{5}{6}\pi, \alpha_4)$ and nearby surfaces bound large volumes. With this in mind, and modifying the curve in the previous section, we choose a five-segment closed loop C as shown in Figure 5(a), which bounds two surfaces S_1 and S_2 parametrized by $(\alpha_1, \alpha_2, \alpha_3, \alpha_4) = (\alpha_1, \alpha_2, \frac{5}{6}\alpha_1, \alpha_2) =: \alpha$ with $D_1 : 0 \leq \alpha_1 \leq \pi, 0 \leq \alpha_2 \leq \frac{1}{2}\pi$, and $(\alpha_1, \alpha_2, \alpha_3, \alpha_4) = (\alpha_1, \frac{1}{2}\pi, \alpha_3, \frac{1}{2}\pi)$ with $D_2 : 0 \leq \alpha_3 \leq \frac{5}{6}\pi, 0 \leq \alpha_1 \leq \frac{6}{5}\alpha_3$.

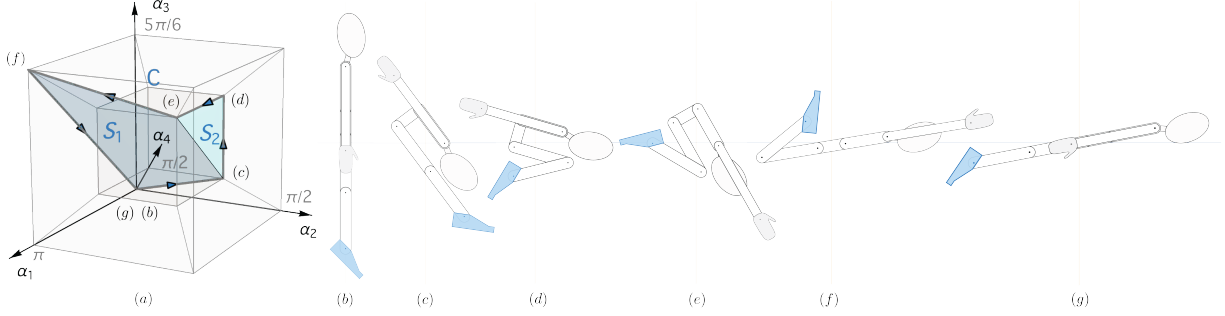


Figure 5: Path C , surfaces S_1 and S_2 , and six configurations of the stick figure during one cycle.

Then (8) reduces to

$$-\int_0^\pi \int_0^{\frac{1}{2}\pi} U_{12}(\alpha) + U_{14}(\alpha) - \frac{5}{6}U_{23}(\alpha) + \frac{5}{6}U_{34}(\alpha) d\alpha_2 d\alpha_1 - \int_0^{\frac{5}{6}\pi} \int_0^{\frac{6}{5}\alpha_3} U_{13}(\alpha_1, \frac{1}{2}\pi, \alpha_3, \frac{1}{2}\pi) d\alpha_1 d\alpha_3, \quad (9)$$

whose numerical value is $1.38165\dots \approx 79.16^\circ$, with contributions of 30.72%, 15.76%, 31.27%, 12.06%, 0%, and 10.19%, from U_{12} , U_{13} , U_{14} , U_{23} , U_{24} , and U_{34} , respectively. In the video <https://youtu.be/NMwIqcHdP6Y>, instead, we have gently shrunk the upper bound $\frac{1}{2}\pi$ for the hip angle α_2 by a factor of 0.911454 such that the orientation change is 72° sharp in one cycle. Thus, it takes 5 cycles to complete a somersault.

The above choices of curves are not optimal. Other dimensions haven't been explored. We hope the reader will find it interesting to continue the expedition among the graph terrains, and also by adding a link here and there. Furthermore, in addition to providing an application of Stokes' Theorems, $\Delta\theta$ is also an example of holonomy [4] for fiber bundles $\mathbb{R}^n \times \mathbb{R}$ with connection and curvature given by (7) and U_{ij} .

Summary. This paper applies Stokes' Theorem and its generalized versions to design choreographic sequences for planar stick figures in free fall and during space walk to perform somersault.

References

- [1] S. J. Di Bartolo, Orientation change of a two-dimensional articulated figure of zero angular momentum. *Am. J. Phys.* **78** (2010) 733-737.
- [2] C. Frohlich, The Physics of Somersaulting and Twisting. *Sci. Am.* **242** (1980) 154-165.
- [3] V. J. Katz, The History of Stokes' Theorem. *Math. Mag.* **52** (1979) 146-156.
- [4] R. Montgomery, *A tour of Subriemannian Geometry*, Mathematical Surveys and Monographs **91**, American Math. Society, Providence, 2006.
- [5] W. Rudin, *Principles of Mathematical Analysis*, 3e. New York: McGraw-Hill, 1976.
- [6] M. Sullivan, Knots about Stokes' Theorem. *College M. J.* **27** (1996) 119-122.